Cell's intrinsic biophysical properties play a role in the systematic decrease in time-locking ability of central auditory neurons

Sungchil Yang[1], **Sunggu Yang**[1], **Charles L. Cox**[1,2], **Daniel A Llano**[1], and **Albert S. Feng**[1]

[1]Department of Molecular and Integrative Physiology & Beckman Institute, University of Illinois at Urbana-Champaign, Urbana Illinois 61801, USA

[2]Department of Pharmacology College of Medicine, University of Illinois at Urbana-Champaign, Urbana Illinois 61801, USA

Abstract

Studies in the vertebrates have shown that the time-locking ability of central auditory neurons decreases progressively along the ascending auditory pathway. This decrease is presumably attributed to a progressive reduction in the fidelity of synaptic transmission and an increase in the influence of synaptic inhibition along the cascade. The extent to which neurons' intrinsic biophysical properties contribute to the change in time-locking ability is unclear. We carried out whole-cell patch clamp recordings from the auditory thalamus of leopard frogs and compared their biophysical properties and time-locking abilities (determined by cell's responses to depolarizing pulse trains applied intracellularly) to those of lower auditory brainstem neurons. We found that frog thalamic neurons were homogeneous, exhibiting uniformly sustained-regular firing patterns, but not having low-threshold transient Ca^{2+} current which mammal thalamic neurons generally possess. Furthermore, intrinsic biophysical properties of the thalamic neurons are such that the time-locking ability of these neurons was very poor. The homogeneity of thalamic auditory neurons is in contrast to the heterogeneity of lower auditory brainstem neurons, with different phenotypes exhibiting different time-locking abilities and with sustained-regular phenotype consistently showing the worst time-locking ability among all biophysical phenotypes. Auditory nuclei along the ascending auditory pathway showed a progressive increase in the population of sustained-regular phenotype – this corresponded to a systematic decrease in the overall time-locking ability, with neurons in the dorsal medullary nucleus showing the best, and thalamic neurons exhibiting the poorest, time-locking ability, whereas neurons in the torus semicircularis displayed intermediate time-locking ability. These results suggest that the biophysical characteristics of single neurons also likely play a role in the change in temporal coding ability along the ascending auditory pathway.

INTRODUCTION

The temporal pattern of sounds is important for sound discrimination in humans (e.g., for speech perception) as well as in various vertebrates and invertebrates (Langner, 1992; Shannon *et al.* 1995). For animals that produce species-specific vocal signals, the temporal

Corresponding author: Sungchil Yang, 210X Barker Hall, Berkeley, CA 94720, University of California at Berkeley, yangs70@berkeley.edu, Tel: 1-510-502-3029, Fax: 1-217-333-1133.

cue is often critical for species recognition. This is best exemplified by call discrimination for two species of gray treefrogs whose advertisement calls have similar spectral characteristics but show distinct temporal properties. Specifically, the rate of amplitude modulation (AM) and the duration and rise/fall times of individual syllables differ between these species (Gerhardt, 2001).

In anurans, the coding of AM stimuli is transformed from a periodicity code in the auditory periphery, to a rate code in the auditory midbrain and thalamus where neurons function as temporal filters and respond selectively to different AM rates (Feng *et al.* 1990; Hall, 1994; Rose and Gooler, 2006). The transformation of the coding scheme is partly attributed to the progressive decrease in time-locking ability of single neurons, from a maximum of 250 Hz at the auditory nerve and dorsal medullary nucleus (DMN, a homolog of the avian and mammalian cochlear nucleus) to <100 Hz at the torus semicircularis (TS, a homolog of the inferior colliculus) (Rose and Capranica, 1985; Feng et al. 1990; Simmons et al. 2000). Responses of neurons in the auditory thalamus to repetitive acoustic stimuli show rapid adaptation with little or no time locking (Feng et al. 1990). Studies in mammals have similarly revealed the progressive decrease in time-locking ability along the central auditory pathway (Fitzpatrick *et al.* 1999; Llano and Feng, 1999; see review by Joris *et al.* 2004). The change in time-locking ability is generally assumed to be due to a decrease in the fidelity of synaptic transmission with increasing numbers of synapses in the cascade, and to an increase in the strength of synaptic inhibition at successive stages of sound processing (Rouiller *et al.* 1979; Rhode and Greenberg, 1992; Feng and Lin 1994; Edwards *et al*. 2007).

There is growing evidence that cell's intrinsic properties contribute to various auditory response properties, including cell's time-locking ability and frequency preference (Llinas, 1988; Oertel, 1999; Hutcheon and Yarom, 2000; Yang *et al.* 2009). For example, the intrinsic membrane properties of neurons (e.g., low input resistance and short membrane time constant) as well as the compositions of ion channels are vitally important for the cell's ability to transmit signals rapidly and precisely (Manis and Marx, 1991; Sivaramakrishnan and Oliver, 2001; Soares *et al.* 2002; Trussel, 1999). To determine whether or not the neurons' intrinsic biophysical properties play a role in the systematic change in time-locking ability of central auditory neurons, we performed *in vitro* whole-cell patch recordings from neurons in the auditory thalamus of Northern leopard frogs, *Rana pipiens pipiens*. We determined their membrane biophysical properties and their entrainment ability in response to depolarizing pulse trains at different repetition rates; these properties were compared to those of lower brainstem neurons (Yang and Feng 2007; Yang *et al.* 2009). Anatomically, the auditory thalamus, which is at the top of the cascade in the frog central auditory system, comprises two divisions: the posterior and central thalamic nuclei. They receive differential innervations from the TS and perform frequency analysis and temporal analysis, respectively (Hall and Feng, 1987; Feng and Lin, 1991). We found that, whereas lower auditory brainstem neurons are heterogeneous, thalamic neurons are homogeneous exhibiting a uniform biophysical phenotype (i.e., giving sustained-regular discharge pattern when membrane was depolarized) that shows the longest membrane time constant and the poorest entrainment ability among all biophysical phenotypes. However, these neurons' dendritic morphology was diverse. These data indicate that the previously-described decrease in temporal precision shown *in vivo* may in part be attributed to the progressive increase in the population of sustained-regular phenotype with their particular intrinsic biophysical properties.

METHODS

Brain slice preparation and electrophysiological recordings

To prepare frog brain slices, young adult northern leopard frogs (*Rana pipiens pipiens*) weighing 10~25 g (6–9 months old) were anesthetized in 0.2 % tricaine methanesulfonate (MS-222, Sigma, St. Louis, MO) and then decapitated. All experiments were done in April to August. Once the brain was extracted, it was immediately placed in an appropriate oxygenated (95 % O_2/5 % CO_2) Ringer solution (in mM) with a pH of 7.6: 104 NaCl, 4 KCl, 1.4 $MgCl_2 6H_2O$, 10 D-glucose, 25 NaHCO$_3$, 2.4 $CaCl_2 2H_2O$. After removal of the dura mater, the tissue was embedded in a 3.2 % solution of low-melting-point agarose (Sigma, St. Louis, MO) dissolved in Ringer solution. After hardening and cooling the agarose block in a freezer (−12°C for 5 ~ 7 min), the block was trimmed to obtain desired slice orientation. The brainstem and forebrain was sectioned along the transverse plane into 300 μm slices using a vibratome (Ted Pella, 1000 plus). Brain slices were immersed in oxygenated Ringer solution in a tissue chamber for <1 hr at room temperature before the electrophysiological recording; the chamber was continuously perfused with Ringer solution at a rate of 2 ml/min.

In this study, we also made a simple comparison of the temporal firing patterns of auditory thalamic neurons in frogs and rats. To prepare rat brain slices, Sprague-Dawley rats (postnatal age: 10–16 days) were deeply anesthetized with sodium pentobarbital (55 mg/kg), the brains were quickly removed and placed into chilled (4°C), oxygenated (5% CO_2 and 95% O_2) slicing medium containing (in mM): 2.5 KCl, 1.25 NaH_2PO_4, 10.0 $MgSO_4$, 0.5 $CaCl_2$, 26.0 NaHCO$_3$, 11.0 glucose, and 234.0 sucrose. The thalamic brain slices were obtained from coronal slices. Slices were transferred to a holding chamber containing oxygenated physiological saline that contained (in mM): 126.0 NaCl, 2.5 KCl, 1.25 NaH_2PO_4, 2.0 $MgCl_2$, 2.0 $CaCl_2$, 26.0 NaHCO$_3$, and 10.0 glucose.

A fixed stage microscope (Olympus BX50WI) equipped with differential interference contrast optics and a 63X water-immersion objective is used to visualize individual neurons. The experimental protocols were reviewed and approved by the University of Illinois Institutional Animal Use and Care Committee (Protocol 05007). Patch electrodes were fabricated from 1.5 mm-diameter borosilicate glass micropipettes and had impedance of 3–6 MΩ when back-filled with the following solution (in mM) having a pH of 7.5–7.6 and osmolarity of 260–270 mOsm: 117 K-gluconate, 13 KCl, 1.0 $MgCl_2 6H_2O$, 0.07 $CaCl_2 2H_2O$, 0.1 EGTA, 10 HEPES, 3 ATP-Mg, 0.3 GTP-Na and 0.3 % biocytin. The initial access resistance typically ranged from 10 to 13 MΩ and remained stable with a series resistance of 9–14 MΩ during the recording session. Neurons showing >15% change in the series resistance were discarded. All recordings were performed at room temperature (~ 22.5°C) using Multiclamp 700B amplifier (Molecular Devices, Sunnyvale, CA). Data were collected and analyzed by means of pCLAMP software (Molecular Devices).

Recording loci

Patch clamp recordings were made from two primary nuclei of the auditory thalamus: the posterior (P) and central (C) nuclei (Neary and Northcutt, 1983; Hall and Feng, 1987). From each frog, we could obtain only 2–3 brain slices (300 μm) that covered the rostrocaudal extent of the posterior and central thalamic nuclei (Fig. 1). Both these nuclei are situated within the dorsal thalamus, and consisted of similarly-sized neurons arranged in vertical laminae; the lateral nucleus, neighboring with posterior and central portions in rostral thalamus, can be distinguished by the lack of lamination and its lower cell density. The boundary between the posterior and central nuclei is characterized by a distinct reduction in cell density. To determine the recording locus, we took a digital photo of the location of the

electrode tip after a neuron's biophysical properties were fully characterized. The locations were substantiated by biocytin staining of recorded neurons. For torus semicirularis (TS) neurons, whole cell-patch clamp recordings were made from all three auditory nuclei of the TS: the principal nucleus (Tp), the laminar nucleus (Tl), and the magnocelluar nucleus (Tmc) (Yang *et al.* 2009).

Biocytin labeling

To identify the locations of the recorded neurons and the cells' morphological characteristics, the cells were filled with biocytin while they were held in whole-cell patch mode. Following the conclusion of patch-clamp recording, we placed the slices in 4 % paraformaldehyde overnight. Slices were then reacted with avidin-biotin-peroxidase complex (ABC Elite, Vector Labs), mounted, and cover slipped with permount (Fisher Scientific, Pittsburgh, PA). Labeled neurons were examined under a light microscope and drawn with the aid of a camera lucida drawing attachment.

Basic membrane properties, firing pattern and entrainment ability

Basic membrane properties and biophysical phenotypes of auditory neurons were determined using the protocols established in an earlier study (Yang and Feng, 2007). The membrane time constant and the input resistance were calculated from the voltage change evoked by small hyperpolarizing current. To determine a cell's biophysical phenotype, we observed its temporal discharge patterns in response to step depolarizing currents (500 ms duration), in 5 ~ 10 pA steps; we also studied the cell's responses to hyperpolarizing currents. The depolarization current was applied to supra-threshold levels sufficient to induce maximal firing, whereas the hyperpolarizing current was applied to a current large enough to evoke negative peak membrane voltage of ~−110 mV.

To investigate the cells' entrainment ability, we examined the cell's response to depolarizing pulses at various repetition rates, from 1 to 250 pulses per second (pps). Five repetitive current pulse trains at near threshold level were presented at various rates; the threshold level was the lowest current intensity (2 ms duration) that could elicit one spike. The numerical results are presented with mean ± SE, unless otherwise stated.

Chemicals

Concentrated stock solutions of pharmacological agents were prepared and diluted in Ringer solution to a final concentration before use. NBQX (10 μM), CPP (10 μM), ZD 7288 (*N*-ethyl-1,6-dihydro-1,2-dimethyl-6-methylimino-*N*-phenyl-4-pyrimidin amine, 50 μM) and TTX (1 μM) were purchased from Tocris (Ellisville, MO). These drugs were bath applied in final concentrations.

RESULTS

Whole cell patch recordings were made from 43 neurons in the posterior (P) and central (C) nuclei of the frog auditory thalamus (Fig. 1a–c). Additionally, we recorded 23 neurons from three nuclei (Tp, Tl, and Tmc) of the torus semicircularis (Fig. 1d).

Biophysical and morphological cell types in the thalamus

Central and posterior thalamic neurons were homogeneous exhibiting a sustained-regular discharge pattern in response to step depolarizing currents – this pattern was characterized by constant inter-spike intervals over the entire duration of current injection, and the inter-spike interval progressively shortened with increasing depolarization current. The responses of central neurons to hyperpolarizing currents were relatively faster compared to those of posterior neurons (Fig 2Ai). As shown in Table 1 and Fig. 2Aii, although central and

posterior thalamic neurons uniformly displayed sustained-regular patterns, two of their intrinsic properties, i.e., their input resistance (Tukey ANOVA, $F_{1,41}$=12.8, $P < 0.01$) and time constant ($F_{1,41}$=6.8, $P = 0.012$), differed significantly for the two nuclei, with posterior neurons showing higher input resistance and longer time constant compared to central neurons.

The morphologies of 21 thalamic neurons (14 in the central nucleus and 6 in the posterior nucleus) across the rostrocaudal extent of the thalamus were characterized in detail. In spite of the uniform temporal firing pattern, we found that their morphology was diverse – this was applicable to both central and posterior nuclei (Fig. 2Bi). Three different soma shapes and dendritic arborization patterns were observed. First was cells showing spherical somata and bipolar or tripolar (with a small appendage) dendritic arborization patterns (Fig. 2Bii; 4 in central nucleus, 2 in posterior nucleus). The 2–3 primary dendrites emanating from the cell body projected in different directions giving rise to multiple but short dendritic bifurcations. The soma size of these spherical cells was large (n = 6, 18.8 ± 2.6 μm) compared to the others (n = 14, 13.9 ± 1.3 μm). Second was neurons exhibiting stellate-shaped somata (Fig. 2Biii; 3 in central nucleus, 2 in posterior nucleus; 15.0 ± 1.2 μm), with multiple primary dendrites emanating from different poles of the soma and projecting in various directions. The third group was characterized by unipolar dendritic arborization patterns (with a small appendage) having minute spherical somata (Fig. 2Biv; 7 in central nucleus, 2 in posterior nucleus; 12.4 ± 1.5 μm). One difference in the dendritic morphology of neurons in the central and posterior nuclei was that the dendrites of central neurons projected exclusively laterally, while the dendrites of some posterior neurons projected toward the midline.

Next, we tested whether frog thalamus neurons have a burst-firing mode driven by low-threshold transient Ca^{2+} (I_T), as commonly observed in thalamic neurons in mammals (Jahnsen and Llinas 1984; Llinas, 1988). As shown in Figure 3A, all rat thalamic neurons tested (n=6) display burst firing riding on their regular firing – this has been shown to be attributable to I_T, a current that tolerates the presence of 1 μM TTX. Surprisingly, we observed no evidence for burst discharges in any frog thalamic neurons (n=4), suggesting that the frog auditory thalamic neurons do not possess I_T. In 4 thalamic neurons, we directly examined the possible occurrence of I_T in the presence of TTX. Under current- and voltage-clamp modes, we could not observe I_T (Fig. 3Bi and Bii)

Comparison of cells' biophysical properties across the auditory brainstem

The intrinsic biophysical properties of thalamic neurons were substantially different from those of lower auditory brainstem that were derived using identical techniques. First, the biophysical properties of neurons in the DMN (Yang and Feng, 2007), and the TS (Yang *et al*. 2009), were heterogeneous (Table 1). In the DMN, neurons displaying onset and onset-like (or phasic-burst) firing patterns in response to step depolarizing currents were the dominant (59 %) biophysical phenotype (Fig. 4A). This phenotype was absent in the thalamus. In contrast, the population of sustained-regular phenotype was low in the DMN (30%) when compared to the thalamus (100%). The populations of onset-like and sustained-regular phenotypes in the TS were intermediate between the DMN and the thalamus, having 11% onset-like phenotype and 38 % sustained-regular phenotype (contrasting to 0% and 100% in the thalamus, respectively), with adapting neurons being the dominant biophysical phenotype (46%). The distributions of biophysical phenotypes in the three different nuclei were significantly different (χ^2= 127, $P < 0.001$).

Second, the input resistance of DMN and TS neurons differed substantially from that of thalamic auditory neurons (Fig. 4B). Whereas the input resistance of the majority of DMN neurons is <200 MΩ, that of TS neurons is between 201 and 1000 MΩ and that of thalamic

neurons was even higher (essentially exclusively >1000 MΩ). As ion channel composition (or distribution) has been shown to contribute to shaping intrinsic membrane properties, e.g., I_h critically contributes to determining the cell's input resistance, and thus to determining the ability to encode temporal features of sound (Pape, 1996; Koch and Grothe, 2003; Yang and Feng, 2007), we additionally measured the magnitude of I_h of thalamic neurons and compared it with those of DMN and TS neurons. In four thalamic neurons, we applied 50 μM ZD 7288 while cells were held in the whole-cell patch voltage-clamp configuration. The effects of ZD 7288 were compared with those of the dominant phenotypes in lower auditory nuclei, e.g., onset neurons in the DMN (n = 4) and adapting neurons in the TS (n = 11) (Fig. 4C). As expected with differential distribution of input resistance of each phenotype, they were significantly different when measured at −100 mV holding (Tukey ANOVA, $F_{2,15}$=10.6, $P < 0.01$).

Entrainment ability

To gain insight into the entrainment ability of auditory thalamic neurons, we studied the cells' responses to depolarizing pulse trains at various repetition rates, in the presence of synaptic blockers (10 μM NBQX for AMPA receptors and 10 μM CPP for NMDA receptors) that eliminated extrinsic influences. We found that, with near-threshold stimulations (1 – 1.2X), a sustained-regular neuron in the central thalamic nucleus could follow depolarization pulses, with 1-1 firing, up to 50 pps. In contrast, a sustained-regular neuron in the posterior nucleus could not follow depolarization pulses even at 3.3 pps (Fig. 5Ai). The pooled data (Fig. 5Aii) indicated that the entrainment ability of central neurons (n = 11; 39 ± 17 pps) appeared superior to that of posterior neurons (n = 3; 4.7 ± 1.8 pps), but the difference was not statistically significant perhaps due to the small sample size from the posterior nucleus (Tukey ANOVA, $F_{1,\,12} = 1.06$, $P = 0.32$).

To compare the time locking ability of thalamic neurons with lower brainstem neurons, we determined the entrainment ability of 23 TS neurons using an identical current injection protocol (for definition of cell's phenotype see Table 1). With near-threshold stimulations, fast-adapting TS neurons (n = 4) exhibited the strongest entrainment ability, with an average cutoff for 1-1 firing of 187 ± 21 pps (Fig 5B) – this was followed sequentially by slow-adapting neurons (n = 9, 151 ± 15 pps), onset-like neurons (n = 2, 100 ± 00 pps), type-I sustained-regulars (n = 4, 79 ± 21 pps), and type-II sustained-regulars (n = 5, 52 ± 18 pps). The entrainment ability of TS neurons was generally higher than that of auditory thalamic neurons.

We also compared the current findings with those reported previously in the DMN (Yang and Feng, 2007). In the DMN, the phasic-burst phenotype has the best entrainment ability (277 ± 28 pps). In the other extreme, sustained-regular neurons in the posterior thalamus exhibited the worst entrainment ability (4.7 ± 1.8 pps) among all auditory neurons in the brainstem. When we compared the best entrainment ability of neurons across the ascending auditory nuclei (Fig. 5C), we found that the best entrainment ability of thalamic neurons, i.e., that of central thalamic neurons, differed significantly from those of phasic-burst and fast-adapting neurons in the DMN and TS, respectively. (Tukey ANOVA, $F_{2,19} = 18.6$, $P < 0.01$). However, the entrainment ability of the sustained-regular phenotype between the auditory nuclei was not significantly different (Fig. 5D, Tukey ANOVA, $F_{2,27} = 1.44$, $P = 0.25$). These results therefore suggest that the gradual decrease of time-locking ability along auditory pathway is in part due to a systematic increase in the number of sustained-regular phenotype.

Discussion

Neurons in the first central auditory station of the anuran, avian and mammals are heterogeneous exhibiting diverse biophysical phenotypes – the heterogeneity allows the auditory system to process the contextual and directional information in parallel (Oertel, 1999; Trussell, 1999; Carr and Soares, 2002; Yang and Feng, 2007). The common biophysical phenotype in the cochlear nucleus (or homologous structures in birds and anurans) is onset and onset-like (phasic-burst) neurons and is characterized by exhibiting one or a few spikes in response to step depolarization currents, irrespective of the current intensity. In light of the rapid channel and receptor kinetics, such neurons have the capacity to faithfully preserve time and phase information in the acoustic signals, making it possible for binaural phase information to be compared and processed in the superior olive. In contrast, the sustained-regular phenotype, characterized by a regular firing pattern in response to depolarization currents, is well suited for processing sound level as they show a wide dynamic response range, and a progressive increase in the firing rate with increasing level of stimulation. Another major phenotype (the adapting neurons) is characterized by a pronounced adaptation in the firing rate responding to step depolarization currents. The intrinsic membrane properties and the time-locking ability of adapting neurons are intermediate between onset-like and sustained-regular neurons.

In frogs, the biophysical properties of neurons in three central auditory structures are now fully characterized: the DMN (the first auditory station; Yang and Feng, 2007), the TS that is a homolog of the mammalian inferior colliculus (Yang *et al.* 2009), and in the present study the auditory thalamus. Surprisingly, frog thalamic auditory neurons are biophysically homogeneous, consisting purely of sustained-regular phenotype.

Results of the present and the earlier *in vitro* studies (Yang and Feng, 2007; Yang *et al.* 2009) show that there is a systematic change in the populations of biophysical phenotypes along the ascending auditory pathway (Table 1). Specifically, whereas the DMN is populated predominately by onset and onset-like phenotypes possessing the strongest entrainment ability, thalamic neurons exclusively comprise sustained-regular phenotype which is characterized by the worst entrainment ability among all biophysical phenotypes. The TS is intermediate between the DMN and the thalamus in terms of the populations of onset-like and sustained-regular phenotypes; its largest population is adapting neurons that possess intermediate entrainment ability. Thus, the two major trends along the frog ascending auditory pathway are: 1. There is a progressive decrease in the population of onset-type biophysical phenotype, 2. There is a progressive increase in the population of sustained-regular phenotype. The increase in the population of sustained-regulars having very poor entrainment ability suggests that the cell's intrinsic membrane properties likely contribute to the steady decrease in sound-evoked time-locking ability.

It has been suggested that pattern of ion channel expression in a neuron is a major contributor to its intrinsic excitability and time locking properties, along with the type of channels and their kinetics (Trussell 1999; Sivaramakrishnan and Oliver, 2001; Carr and Soares, 2002; Yang and Feng, 2007). Many neurons in auditory nuclei possess I_h current which does not merely determine membrane properties (lowering the membrane resistance), but also transforms the cell's firing pattern (Pape, 1996; Oertel 1999; Yang et al. 2009). Like I_h, the inwardly rectifying potassium channel (I_{kir}) and the low-threshold potassium channel (I_{kl}) contribute significantly to cell's intrinsic membrane properties and thus to the precision in signal transmission. Interestingly, the sustained-regular phenotype in the DMN and TS generally show only minute amounts of I_h, I_{kir} and I_{kl} – this finding may extend also to the sustained-regular phenotypes in the thalamus. As all thalamic neurons have high input resistance and long time constant, perhaps due in part to reduced amounts of I_h, I_{kir} and I_{kl},

their inferior time-locking ability makes them unsuitable for precise periodicity coding (this function is largely carried out in lower auditory nuclei), giving them mainly the rate code for encoding amplitude modulated stimuli.

In contrast, in mammals, thalamic neurons commonly display burst firing with low-threshold Ca^{2+} spikes which promotes the relaying of time-locked activity to the auditory cortex (Jahnsen and Llinas 1984; Llinas, 1988; Guillery & Sherman, 2002; Llinas & Steriade, 2006; Wallace *et al.*, 2007). Llinas and Steriade (2006) further reported that thalamic neurons in all vertebrates, including amphibians (without specifying the recording region), possess a bursting mode. We, however, did not find any neurons with a low-threshold Ca^{2+}-mediated burst-firing mode. Thus, the burst-firing pattern is likely a property of neurons in thalamic regions other than the posterior and central nuclei.

It has previously been suggested that multiple synapses may not always contribute to inferior time-locking ability of neurons in higher auditory centers. The strength of time locking can actually be enhanced or retained by the convergence of synaptic inputs (Langner, 1992; Joris *et al.* 1994; Wallace *et al.* 2007). An implication of the above tenet is that, systematic changes in cells' intrinsic properties along the ascending auditory pathway, as shown here with the frog's central auditory system, may be an important contributor to the systematic decrease in time locking ability.

In vivo studies in the mammalian medial geniculate body showed that phase-locking is unit- and region-specific, with units in the medial division showing a similar upper limit of phase-locking as units in the inferior colliculus, and units in the ventral division showing a lower upper limit, much like units in the primary auditory cortex (Wallace *et al.* 2007); these investigators did not test the individual cells' ability to process synaptic transmission (e.g., synaptic jitter) nor determine the cell's intrinsic membrane properties. Interestingly, we also found that the two divisions of frog thalamus show differential time-locking ability. Our studies further show that this difference is at least in part attributed to differences in cells' intrinsic biophysical properties.

In lower auditory nuclei, cells' firing patterns tend to correspond to their morphology (Rhode *et al.* 1983, Cant, 1992; Rhode and Greenberg, 1992; Carr and Soares, 2002; Yang and Feng, 2007). For the frog thalamus, the dendritic morphology of a single biophysical phenotype is diverse, and thus there is no 1-1 correspondence. The heterogeneity of the dendritic morphology does not appear to account for the functional dichotomy of the frog auditory thalamus (e.g., the posterior and central nuclei are devoted to spectral and time-domain processing, respectively) (Hall and Feng, 1987). On the other hand, our finding that neurons in the posterior nucleus have higher input resistance and longer time constant than those in the central nucleus may contribute to the functional dichotomy, as the very high input resistance of sustained-regulars in the posterior nucleus is not suited for time-domain processing. Nonetheless, this hypothesis requires experimental validation through *in vivo* patch clamp studies.

Acknowledgments

References

Cant, NB. The cochlear nucleus: Neuronal types and their synaptic organization. In: Webster, DB.; Popper, AN.; Fay, RR., editors. The Mammalian Auditory Pathway: Neuroanatomy. Springer-Verlag: New York; 1992. p. 66-116.

Carr CE, Soares D. Evolutionary convergence and shared computational principles in the auditory system. Brain Behav Evol. 2002; 59:294–311. [PubMed: 12207085]

Edwards CJ, Leary CJ, Rose GJ. Counting on inhibition and rate-dependent excitation in the auditory system. J Neurosci. 2007; 27:13384–13392. [PubMed: 18057196]

Feng AS, Hall JC, Gooler DM. Neural basis of sound pattern-recognition in anurans. Progress in Neurobiology. 1990; 34:313–329. [PubMed: 2185497]

Feng AS, Lin WY. Differential innervation patterns of three divisions of frog auditory midbrain (torus semicircularis). J Comp Neurol. 1991; 306:613–630. [PubMed: 1712796]

Feng AS, Lin WY. Phase-locked response characteristics of single neurons in the frog cochlear nucleus to steady-state and sinusoidal-amplitude-modulated tones. J Neurophysiol. 1994; 72:2209–2221. [PubMed: 7884454]

Fitzpatrick DC, Kuwada S, Kim DO, Parham K, Batra R. Responses of neurons to click-pairs as simulated echoes: Auditory nerve to auditory cortex. J Acoust Soc Am. 1999; 106:3460–3472. [PubMed: 10615686]

Gerhardt, HC. Acoustic communication in two groups of closely related treefrogs. In: Slater, PJB.; Rosenblatt, JS.; Snowdon, CT.; Roper, TJ., editors. Advances in Behavioral Biology. Academic Press; New York: 2001. p. 99-167.

Guillery RW, Sherman SM. Thalamic relay functions and their role in corticocortical communication:generalizations from the visual system. Neuron. 2002; 33:163–175. [PubMed: 11804565]

Hall JC. Central processing of communication sounds in the anuran auditory system. Amer Zool. 1994; 34:670–684.

Hall JC, Feng AS. Evidence for parallel processing in the frog's auditory thalamus. J Comp Neurol. 1987; 258:407–419. [PubMed: 3495555]

Hutcheon B, Yarom Y. Resonance, oscillation and the intrinsic frequency preferences of neurons. Trends Neurosci. 2000; 23:216–222. [PubMed: 10782127]

Jahnsen H, Linas R. Electrophysiological properties of guinea-pig thalamic neurons: an in vitro study. J Physiol. 1984; 349:205–226. [PubMed: 6737292]

Joris PX, Schreiner CE, Rees A. Neural processing of amplitude-modulated sounds. Physiol Rev. 2004; 85:541–577. [PubMed: 15044682]

Joris PX, Carney LH, Smith PH, Yin TCT. Enhancement of neural syschronization in the anteroventral cochlear nucleus. I Responses to tones at the characteristic frequency. J Neurophysiol. 1994; 71:1022–1036. [PubMed: 8201399]

Koch U, Grothe B. Hyperpolarization-activated current (Ih) in the inferior colliculus: distribution and contribution to temporal processing. J Neurophysiol. 2003; 90:3679–3687. [PubMed: 12968010]

Llano DA, Feng AS. Response characteristics of neurons in the medial geniculate body of the little brown bat to simple and temporally-pattern sounds. J Comp Physiol. 1999; 184:371–385. [PubMed: 10377974]

Langner G. Periodicity coding in the auditory-system. Hear Res. 1992; 60:115–142. [PubMed: 1639723]

Llinas RR. The intrinsic electrophysiological properties of mammalian neurons: insights into central nervous system function. Science. 1988; 23:1654–1664. [PubMed: 3059497]

Llinas RR, Steriade M. Bursting of thalamic neurons and states of vigilance. J Neurophyiol. 2006; 95:3297–3308.

Neary TJ, Northcutt RG. Nuclear organization of the bullfrog diencephalon. J comp Neurol. 1983; 213:262–278. [PubMed: 6601115]

Manis PB, Marx SO. Outward currents in isolated ventral cochlear nucleus neurons. J Neurosci. 1991; 11:2865–2880. [PubMed: 1880553]

Oertel D. The role of timing in the brain stem auditory nuclei of vertebrates. Ann Rev Physiol. 1999; 61:497–519. [PubMed: 10099699]

Pape HC. Queer current and pacemaker: the hyperpolarization-activated cation current in neurons. Annu Rev Physiol. 1996; 58:299–327. [PubMed: 8815797]

Rhode, WS.; Greenberg, S. Physiology of the cochlear nuclei. In: Popper, AR.; Fay, RR., editors. The Mammalian Auditory Pathway: Neurophysiology. Springer-Verlag; New York: 1992. p. 94-152.

Rhode WS, Smith PH, Oertel D. Physiological response properties of cells labeled intracellularly with horseradish peroxidase in cat dorsal cochlear nucleus. J Comp Neurol. 1983; 213(4):426–47. [PubMed: 6300199]

Rose GJ, Capranica RR. Sensitivity to amplitude modulated sounds in the anuran auditory nervous system. J Neurophysiol. 1985; 53:446–465. [PubMed: 3872351]

Rose, GJ.; Gooler, DM. Function of the amphibian central auditory system. In: Narin, P.; Feng, AS.; Fay, RR.; Popper, A., editors. Hearing and sound communication in amphibians. Springer-Verlag; New York: 2006. p. 250-290.

Rouiller E, De ribaupierre Y, De ribaupierre. Phase-locked responses to low frequency tones in the medial geniculate body. Hear Res. 1979; 1:213–226.

Shannon RV, Zeng FG, Kamath V, Wygonski J, Ekelid M. Speech recognition with primarily temporal cues. Science. 1995; 270:303–304. [PubMed: 7569981]

Simmons AM, Sanderson MI, Carabedian CE. Representation of waveform periodicity in the auditory midbrain of the bullfrog, *Rana catesbeiana*. J Assoc Res Otolaryngol. 2000; 1:002–024.

Sivaramakrishnan S, Oliver DL. Distinct K currents result in physiologically distinct cell types in the inferior colliculus of the rat. J Neurosci. 2001; 21:2861–2877. [PubMed: 11306638]

Soares D, Chitwood RA, Hyson RL, Carr CE. Intrinsic neuronal properties of the chick nucleus angularis. J Neurophysiol. 2002; 88:152–162. [PubMed: 12091541]

Trussell LO. Synaptic mechanisms for coding timing in auditory neurons. Ann Rev Physiol. 1999; 61:477–496. [PubMed: 10099698]

Wallace MN, Anderson LA, Palmer AR. Phase-locked response to pure tones in the auditory thalamus. J Neurophysiol. 2007; 98:1941–1952. [PubMed: 17699690]

Yang S, Feng AS. Heterogeneous biophysical properties of frog dorsal medullary nucleus (cochlear nucleus) neurons. J Neurophysiol. 2007; 98:1953–1964. [PubMed: 17686915]

Yang S, Lin WY, Feng AS. Wide-ranging frequency preferences of auditory midbrain neurons: Roles of membrane time constant and synaptic properties. Eur J Neurosci. 2009; 30:76–90. [PubMed: 19558621]

Highlight

Frog thalamic neurons are homogeneous displaying regular firing pattern, but heterogeneous morphology.

Thalamic neurons show poor entrainment ability compared to lower auditory neurons.

It implicates progressive decrease of time-locking ability along auditory pathway.
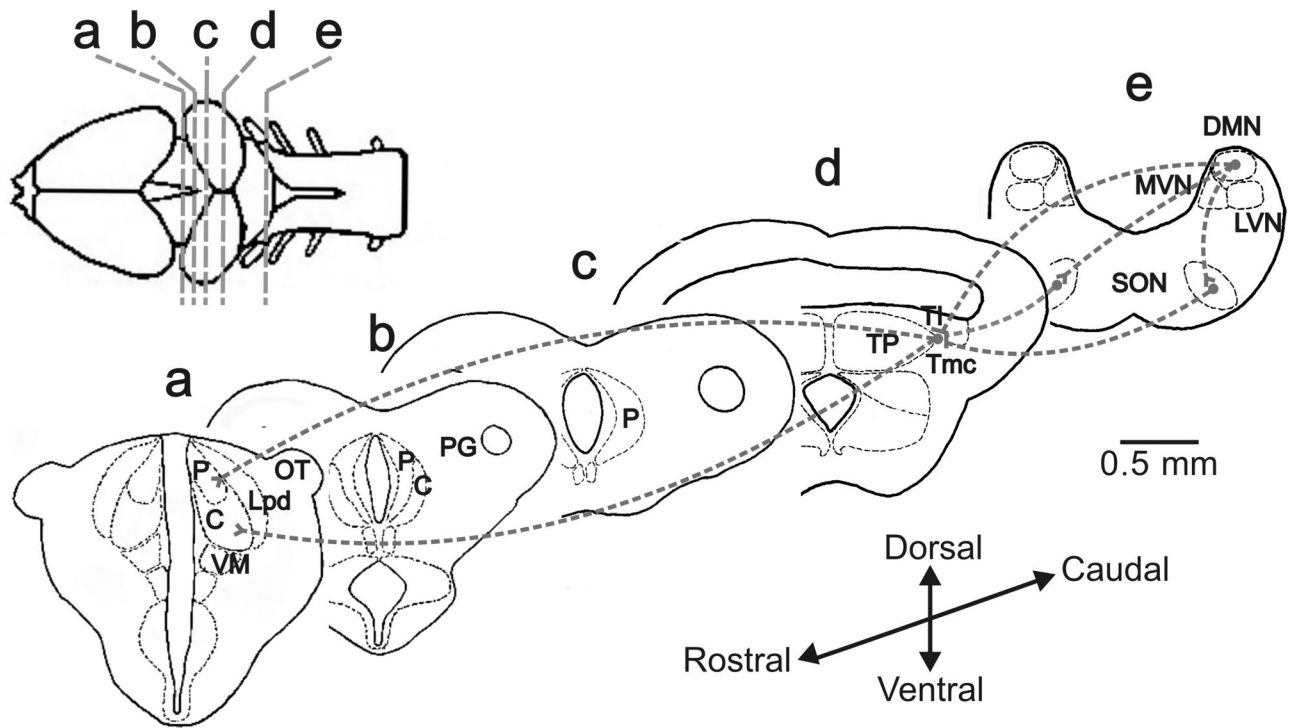
Figure 1.
Schematic diagram of frog brain showing its dorsal view and its transverse sections (along with various main auditory nuclei) at respective rostrocaudal extent of the brain. Panels a, b and c show the locations of the posterior and central nuclei of the auditory thalamus; panels d and e display the locations of the torus semicircularis (TS) and caudal brainstem nuclei, respectively. The gray arrows show the primary ascending projection pattern – this is the simplified version as the projections shown ignore the laterality of these connections. Abbreviation: C, central thalamic nucleus; DMN, dorsal medullary nucleus; Lpd, posterodorsal division of the lateral thalamic nucleus; OT, optic tectum; P, posterior thalamic nucleus; PG, pretectal gray; SON, superior olivary nucleus; Tl, laminar nucleus of the TS; Tmc, magnocellular nucleus of the TS; Tp, principal nucleus of the TS.
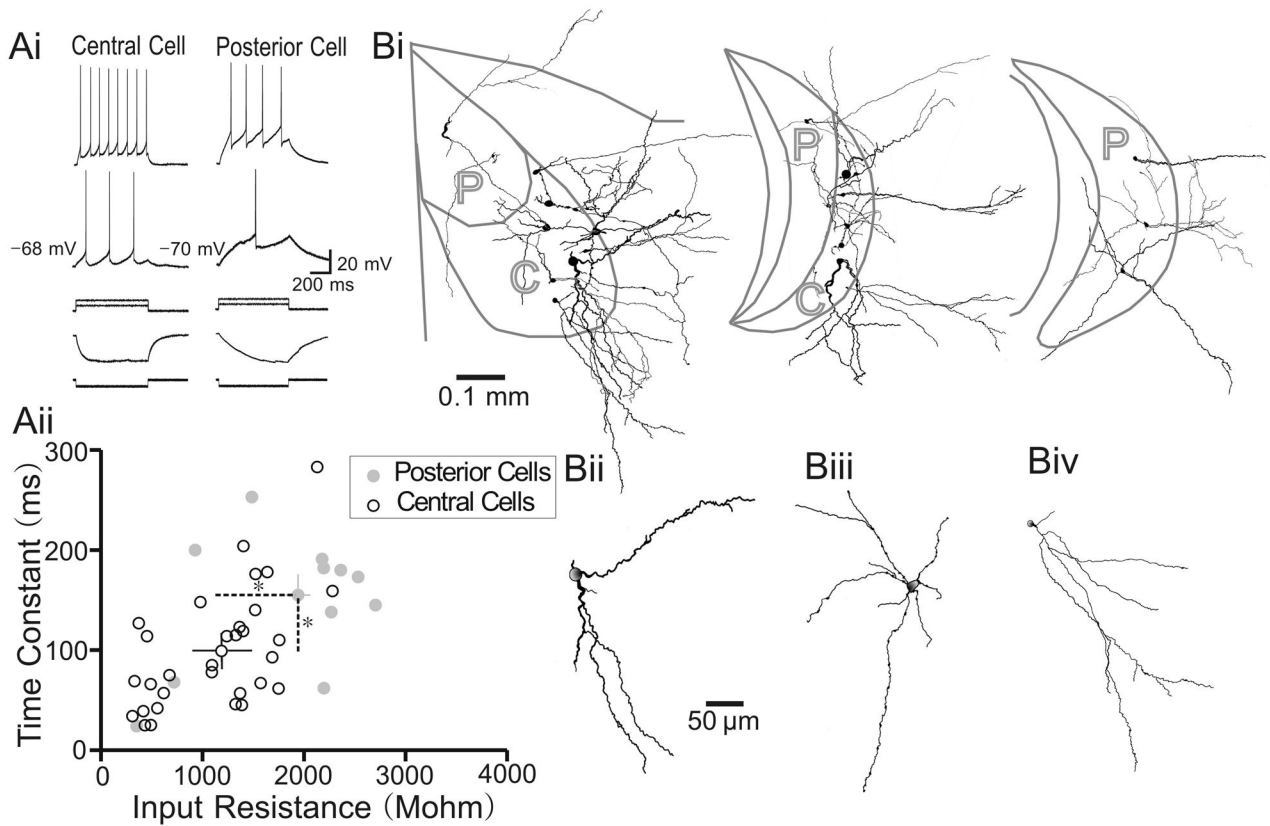
Figure 2.
Representative sustained-regular phenotypes in the central and posterior nuclei of the auditory thalamus. Ai. Responses to step depolarizing currents of 60 and 30 pA for a central thalamic neuron (20 and 10 pA for a posterior thalamic neuron) are characterized by constant inter-spike intervals; the fourth trace shows the response to a hyperpolarizing step-current of −30 pA for the central thalamic neuron (−10 pA for the posterior thalamic neuron). Aii. Distribution of the time constant of thalamic neurons as a function of their input resistance. The time constant and the input resistance of central thalamic neurons differ from those of posterior thalamic neurons. B. Biocytin-filled sustained-regulars with different dendritic arborization patterns. Sustained-regulars show heterogeneous morphological phenotypes: bipolar (Bii), multipolar(Biii), and unipolar (Biv). Abbreviation: C, central thalamic nucleus; P, posterior thalamic nucleus. *$P < 0.05$.
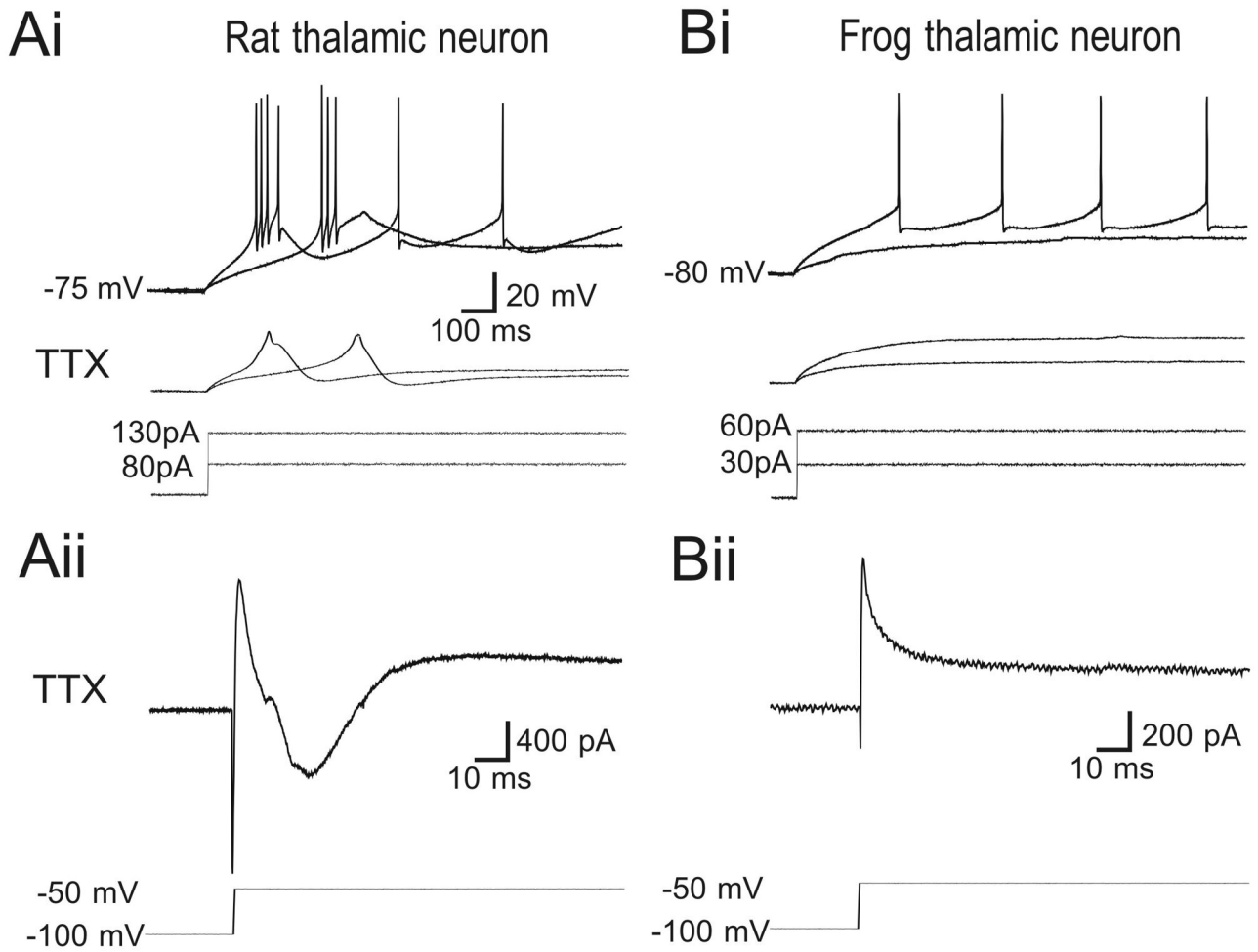
Figure 3.

Absence of I_T in frog thalamic neurons. In contrast to rat thalamic neurons, frog thalamic neurons did not show low-threshold Ca^{2+}-mediated inward current (I_T) in both the current clamp (Ai) as well as the voltage clamp mode (Aii), respectively.
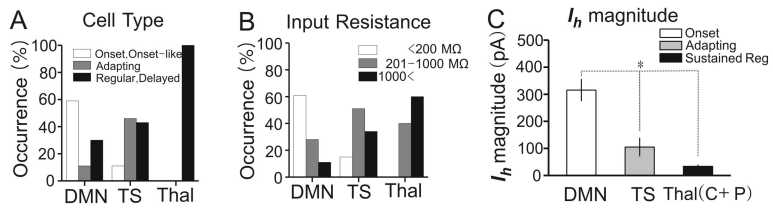
Figure 4.
Comparison of the distributions of biophysical phenotypes (A), membrane input resistance (B), and I_h magnitude (C) of neurons in the DMN, TS and auditory thalamus. Abbreviation: C, central thalamic nucleus; P, posterior thalamic nucleus. $*P < 0.05$.
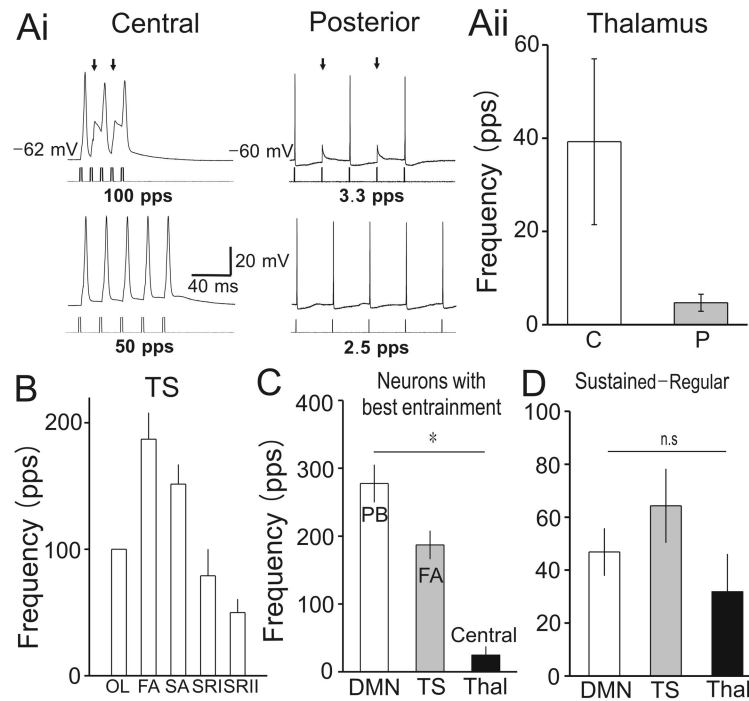
Figure 5.
Neurons in the DMN, TS and auditory thalamus exhibit differential entrainment abilities. Ai. Responses to repetitive depolarizing pulses at near threshold level from central and posterior thalamic neurons. Arrows point to subthreshold voltage responses. Aii. Pooled data from central and posterior sustained-regulars. B. Entrainment ability of five biophysical phenotypes in the TS. C & D. Comparison of the entrainment ability across the DMN, TS and auditory thalamus. Comparison of the entrainment ability of the biophysical phenotypes with the best entrainment ability in each auditory station is shown in C. Comparison of the entrainment ability of sustained-regular in the DMN, TS and thalamus is shown in D. Error bars represent standard error. Abbreviation: C, Central; P, Posterior; OL, onset-like; FA, fast-adapting; SA, slow-adapting; SRI, sustained-regular type- I; SR II, sustained-regular type-II. Abbreviation: PB, phasic-bursting; ON, onset. *$P < 0.05$; n.s., not significant.

Table 1

Shown are biophysical phenotypes (with two intrinsic membrane characteristics) and their distributions along the frog central auditory pathway (Yang & Feng, 2007 for DMN; Yang et al., 2009 for TS).

Biophysical characteristics of frog central auditory neurons

Regions	Cell types		Input Resist. (Mohm)	Time Const. (ms)	Distribution (%)	Firing pattern
	Onset	Type-I	44 ± 17	1.3 ± 0.8	20%	
		Type-II	142 ± 30	4.0 ± 1.6	19%	
	Phasic-burst		156 ± 67	5.1 ± 2.4	20%	
DMN	Adapting		208 ± 75	7.2 ± 4.8	11%	
	Sustained-R	Type-I	306 ± 116	12.9 ± 5.5	21%	
		Type-II	2579 ± 484	79.9 ± 26.2	9%	
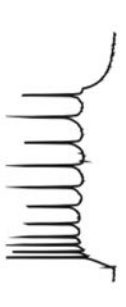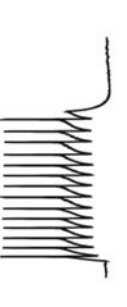
Biophysical characteristics of frog central auditory neurons

Regions	Cell types		Input Resist. (Mohm)	Time Const. (ms)	Distribution (%)	Firing pattern
	Onset-like		56 ± 15	1.5 ± 0.7	11%	
	Adapting	Fast	186 ± 82	6.0 ± 4.2	10%	
		Slow	719 ± 317	32 ± 15	36%	
TS	Sustained-R	Type-I	1079 ± 252	78 ± 35	23%	
		Type-II	2422 ± 912	135 ± 53	15%	
	Delayed		974 ± 383	51 ± 9	5%	
Thalamus	Sustained-R	Central	1128 ± 101	99 ± 11	100%	
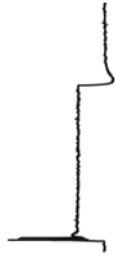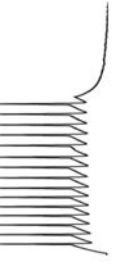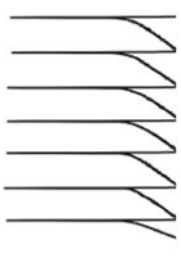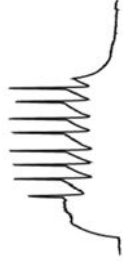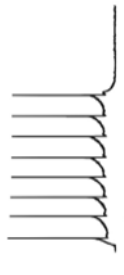
Biophysical characteristics of frog central auditory neurons

Regions	Cell types	Input Resist. (Mohm)	Time Const. (ms)	Distribution (%)	Firing pattern
Sustained-R	Posterior	1940 ± 256	155 ± 21	100%	
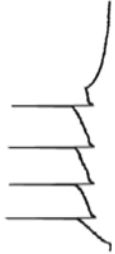
Abbreviation: DMN, dorsal medullary nucleus; TS, torus semicircularis; Sustained-R, Sustained-Regular; Input Resist., Input Resistance; Time Const., Time Constant. The classification was based on the cell's temporal firing pattern in response to step depolarizing currents having a duration of 250 ms (onset phenotypes gives one spike only; phasic-burst gives a few spikes over the first 10–15 ms of current stimulation; adapting phenotype gives a series of spikes over much of the duration of current stimulation, with some showing rapid and others exhibiting slow adaptation; sustained-regular phenotype display continuous firing over the entire duration of current stimulation with a constant inter-spike interval). Type-I and type-II onset phenotype and sustained-regular phenotype represent subtypes of these respective phenotypes, in light of the bimodal distribution in their input resistance and membrane time constant.